Synthesis and Characterization of Cross-linked Sulfonated Polystyrene Nanoparticles

4 AUTHORS, INCLUDING:

Steven Swier
Dow Corning Corporation
32 PUBLICATIONS **744** CITATIONS

SEE PROFILE

R. A. Weiss
University of Akron
227 PUBLICATIONS **5,205** CITATIONS

SEE PROFILE

Synthesis and Characterization of Cross-linked Sulfonated Polystyrene Nanoparticles

Smita B. Brijmohan,[†] Steven Swier,[†,§] R. A. Weiss,[†,‡] and Montgomery T. Shaw*,[†,‡]

Polymer Program, Institute of Materials Science and Department of Chemical Engineering, University of Connecticut, Storrs, Connecticut 06269

Cross-linked polystyrene particles have applications in many fields such as ion exchange columns, fuel cell membranes, and catalysis, to name a few. Synthesis of these particles in smaller sizes offers various advantages due to the increased specific surface area. Polystyrene nanoparticles having volume-equivalent diameters in the range of 40−60 nm were synthesized using emulsion polymerization. Emulsifier-free synthesis was also employed, yielding particles in the size range of 80−90 nm. Sodium styrene sulfonate (NaSS) was used an emulsifying comonomer, and divinyl benzene (DVB) was used as a cross-linking agent. The average particle diameter increased with increasing DVB concentration in the feed. By increasing the NaSS content in the feed from 4 to 28 wt %, the ion exchange capacity of the cross-linked polystyrene particles increased from 0.05 to 2.2 meq/g. The presence of SO_3Na groups in the cross-linked polystyrene particles was also confirmed by using FT-IR, and the intensity of the peaks at 1040 and 1182 cm^{-1} increased with increasing NaSS concentration in the feed.

1. Introduction

Ion-exchange resins of cross-linked polystyrene sulfonic acid (SXLPS) have been used in various applications. The more significant applications include water purification, catalysis,[1−5] separation of catalyst from polymer[6,7] synthesis of magnetic particles,[8] and chromatography.[9,10] These resins have been synthesized in various forms such as porous beads, microparticles, and continuous columns, depending on the final application. More recently micron-size particles of SXLPS have found application as proton-conducting components in polymeric fuel cell membranes.[11−15] Most applications of SXLPS, especially the latter, require the resin particles to be highly sulfonated on the surface. The effective ion-exchange capacity (IEC), which is a measure of the level of sulfonation, generally increases with increasing specific surface area because internal ion clusters may be less accessible to exchange, at least at the lower values of the IEC.

Various methods for synthesizing cation-exchange resins have been reported in the literature and most involve sulfonation of polymerized particles.[16] The most commonly used method is suspension polymerization,[17−19] where water is used as suspending medium to disperse droplets of monomers. The initiator is soluble in the monomer, and the reaction progresses as bulk polymerization within the microreactors formed by monomer droplets. The particle size obtained by this type of polymerization is in the range of 10 μm to 1 mm. Another well-known technique to obtain polymers in the form of beads or particles is emulsion polymerization.[20,21] In this polymerization, the monomer droplets are stabilized by micelles formed by the surfactant or emulsifier, which also stabilizes the polymer particles after the reaction. An important difference between suspension and emulsion polymerization is that for the latter the initiator is water soluble. Particles with diameters as low as 40 nm can be synthesized by emulsion polymerization.[21] As an example, Turner et al.[22] demonstrated the synthesis of a copolymer of styrene and sodium styrene sulfonate (NaSS) by emulsion polymerization and found that in the presence of NaSS, the rate of copolymerization was higher than styrene homopolymerization by the same method. Also, they reported that the presence of the ionic sodium styrene sulfonate groups on the particle surface made the particles more dispersible in water. The technique of emulsifier-free synthesis has been employed with the use of surface-active initiators[23] or stabilizing comonomers such as ethyl acrylate[24] or NaSS.[25−27] They form an ionic charge over the monomer droplets or polymer particles, thereby stabilizing the system. The stabilizing comonomers reportedly increase the polymerization rate.

In this paper, we describe the synthesis and characterization of SXLPS nanoparticles by emulsion and emulsifier-free polymerization. Previous work by other authors[22,25] dealt mainly with the effect of NaSS on polymerization rate to linear polystyrene. In the present study, divinyl benzene (DVB) was used as the cross-linking agent, and NaSS was used as an additional stabilizing comonomer in order to form an ionic charge on the surface of the nanoparticles. The amounts of DVB and NaSS in the feed were varied to find their effects on particle size, its distribution, and ion exchange capacity. The emulsifier-free procedure helped in eliminating the use of emulsifier in the reaction, and NaSS solely acted as a stabilizer for the particles. The advantage of emulsifier-free polymerization lies in its "one stage" procedure for obtaining sulfonated cross-linked polystyrene. The properties of particles synthesized by the two methods are presented and compared. A convenient empirical function was used to describe

---

* To whom correspondence should be addressed. E-mail: Montgomery.shaw@uconn.edu.

† Polymer Program, Institute of Materials Science.

‡ Department of Chemical Engineering.

§ Present address: Dow Corning Corporation, 2200 W. Salzburg Rd, Midland, MI 48686.

Table 1. Formulations for Cross-Linked Polystyrene Nanoparticles Synthesis

sample ID	styrene wt fraction[a]	sodium styrene sulfonate (NaSS) wt fraction	divinyl benzene (DVB) wt fraction	sodium dodecyl sulfate (SDS), pph with respect to	
				monomers	water
E1	0.833	0.167	0	5.33	2.67
E2	0.938	0.038	0.025	6.00	2.67
E3	0.816	0.163	0.021	5.22	2.67
E4	0.917	0.037	0.046	5.87	2.67
E5	0.800	0.160	0.040	5.12	2.67
E6	0.769	0.154	0.077	4.92	2.67
N1	0.800	0.160	0.040	0	0
N2	0.690	0.276	0.034	0	0

[a] Weight fraction calculated on basis of total feed weight of all monomers.

the trend in the IEC with increasing NaSS weight fraction in feed.

2. Experimental Section

2.1. Materials. Styrene (Fisher Chemicals) and DVB (Aldrich, 80% mixture of isomers) were washed with a 10% solution of sodium hydroxide (NaOH) in water to remove the inhibitor. After washing three times with the NaOH solution, the monomers were washed with deionized (D.I.) water. 4-Styrenesulfonic acid, sodium salt hydrate (NaSS), dodecyl sulfate, sodium salt (SDS) (98%), a surfactant, potassium persulfate ($K_2S_2O_8$) initiator, and a chain-transfer agent n-dodecyl thiol ($C_{12}H_{25}SH$) were used as received from Aldrich. A 1% solution of hydroquinone (Aldrich) in water was used to terminate the polymerization reaction.

The solutions for determination of ion exchange capacity were prepared as follows. A 0.5 M solution of hydrochloric acid (HCl) was prepared by volumetric dilution of a 36.5 wt % HCl solution (J. T. Baker). A 0.01 M solution of NaOH was prepared by volumetric dilution of a 0.1 M standard solution (Alfa Aesar). A 20% solution of sodium chloride (NaCl) salt (Fisher Scientific) was prepared in deionized water.

2.2. Synthesis of Cross-linked Polystyrene Nanoparticles. The formulations for various batches of polystyrene synthesis are compiled in Table 1. The reactions for all the batches were carried out in 250-mL Erlenmeyer flasks equipped with magnetic stir bars of similar size and shape. The flasks were charged with 60 mL of deionized (D.I.) water and NaSS as per formulation. After complete dissolution of NaSS in water, styrene, DVB, and SDS (for batches E1−E5), 0.1 g of n-dodecyl thiol and 0.1 g of potassium persulfate were added. The flasks were capped with a rubber septum, and nitrogen gas was purged through each one for 5 min. The flasks were then placed in a water bath maintained at 60 °C, and the reaction was carried out with constant agitation for 6 h for the emulsion polymerizations (E1−E6) and for 21 and 42 h for the emulsifier-free polymerizations N2 and N1, respectively. The reaction times for N1 and N2 were arbitrarily chosen; during the first 6 h of the reaction, the reaction mixture still appeared clear, whereas toward the end of the reaction time, it became white. Toward the end of the reaction, the mixture in the flask thickened and was difficult to stir. A 3-mL aliquot of the 10% hydroquinone solution was added to stop the reaction.

Following the reaction, the contents of the flask were transferred into cellulose dialysis tubing (pore diameter = 4.8 nm) that was placed in a beaker containing D.I.

water. Dialysis was carried out for 4−5 days, with water being replaced several times to ensure removal of all the salts and unreacted monomers from the product. The product was dried in a vacuum oven at 100 °C for 6 h. A schematic of the polymerization reaction is shown in Figure 1.

2.3. Transmission Electron Microscopy. Particle sizes were determined from the images obtained with a Philips 420 transmission electron microscope (TEM) (80 kV). Samples taken from the emulsion solution were diluted to 0.001 g/mL, and a 3-μL drop was placed on carbon-coated grids and allowed to slowly dry at room temperature.

2.4. Infrared Spectra. The FT-IR spectra of polymer samples were obtained with a Nicolet Magna IR 560 spectrometer. Typically, 1−2-mg samples were mixed with 100 mg of potassium bromide powder and pressed into pellets. All the spectra represent an average of 32 scans taken in the wavenumber range of 4000−400 cm^{-1}.

2.5. Ion Exchange Capacity. The ion exchange capacity (IEC) of the synthesized polystyrene particles was measured by titration. Typically, 0.5 g of sample was treated with 10 mL of 0.5 M HCl and stirred for 1 day. The sample was then dialyzed to remove any excess acid and salt. After drying in a vacuum oven for 4 h, 0.1 g of the sample was treated with 20 mL of 20% NaCl solution for 6 h to exchange all the H$^+$ ions with Na$^+$. The HCl formed as a result of this ion exchange was titrated with 0.01 M NaOH using phenolphthalein as the indicator.

3. Results and Discussion

3.1. Particle Size. The TEM images of the cross-linked polystyrene nanoparticles synthesized by emulsion polymerization are shown in Figure 2. The average diameter representing the volume equivalent diameter was calculated as it is appropriate for phenomena that depend on volume fraction. The volume-average diameter was calculated from

$$D = \left[\frac{\sum_{i=1}^{N_{bins}} n_i d_i^3}{\sum_{i=1}^{N_{bins}} n_i} \right]^{1/3} \quad (1)$$

where D = volume equivalent diameter and n_i = the number of particles in the bin with diameter $d_i \pm \Delta d/2$ where Δd is $d_i - d_{i-1}$.

The particle diameters were also fitted using a normal distribution, the statistics for which are listed in Table 2. In the literature one finds contradicting statements concerning the dependence of particle size on the extent of cross-linking. Barar et al.[18] reported that the particle size decreases with an increase in cross-link density, whereas Bai et al.[28] recently reported that an increasing cross-link density increases the particle diameter. Yang et al.[29] observed no change in the particle diameter with increasing cross-link density. We observed an increasing diameter with increasing DVB concentration in experiments where the reaction conditions and all the components of the feed were kept constant, as long as the weight fraction of NaSS was in the range of 0.16 ± 0.007 (Figure 3; $p = 0.05$ for the trend, where p represents
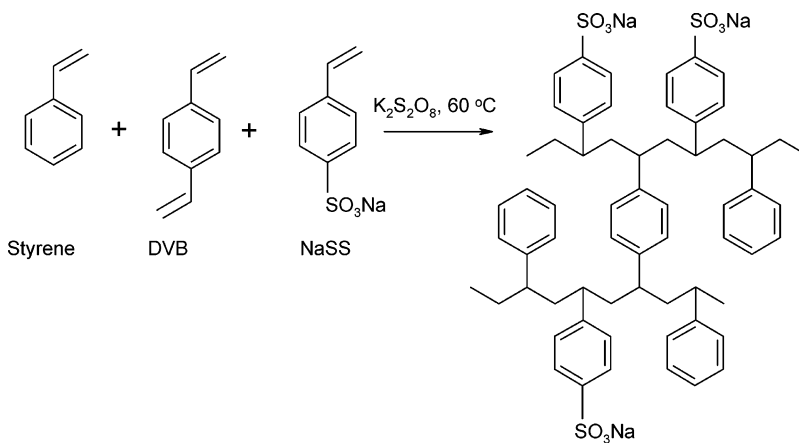
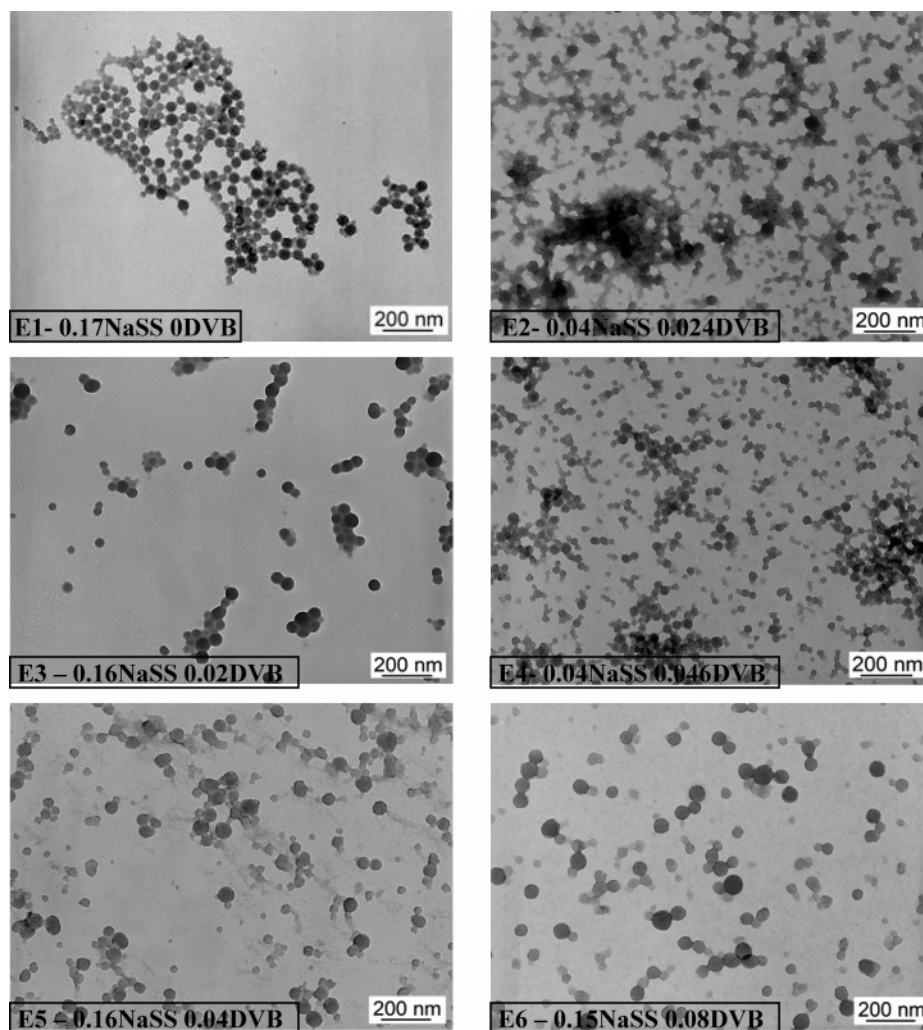**Figure 1.** Schematic of polystyrene synthesis reaction.

Figure 2. TEM images of cross-linked polystyrene nanoparticles prepared with various formulations by using emulsion polymerization.

the probability of type I error in statistical estimation or hypothesis testing). These results agree with the findings reported by Bai et al., who explained this in terms of the solubility parameters of the monomers in the solvent. The cross-linked oligomers from DVB, being insoluble in water, precipitate readily on the nuclei of particles and hence increase the particle size. The higher weight fractions of DVB contribute to more oligomers precipitating on the nuclei. The DVB can also play an important role in inter-cross-linking between the precursor particles. The distribution statistics in

Table 2 indicate a high polydispersity in the samples, which can be attributed to the viscosity build-up toward the end of reaction and the effect of the stabilizing comonomer. In a similar work by Kim et al.[25] it was reported that high concentrations of NaSS resulted in broad particle size distributions.

According to the classical theories of Smith[30] and Ewart et al.[31] for emulsion polymerization of styrene, a large surfactant concentration results in a large number of polymer particles. The micelles formed by the surfactant initially stabilize the monomer droplets and then
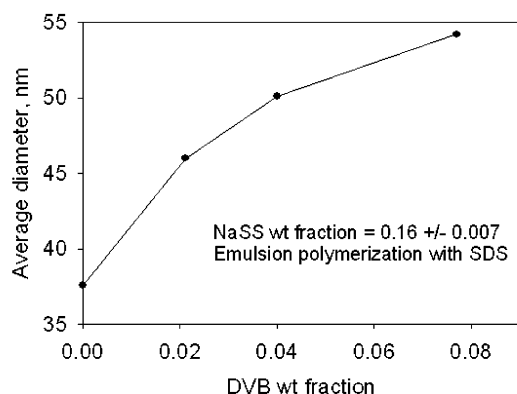
Figure 3. Effect of DVB concentration in emulsion polymerization feed on the average particle diameter with all the components constant. ($p = 0.05$ for the increasing trend.)

Table 2. Volume Equivalent Particle Diameter

sample ID	number of particles	average particle diameter (volume equivalent), nm	std dev
E1	35	37.6	5.57
E2	30	40.0	11.7
E3	20	46.0	11.1
E4	20	31.5	8.0
E5	49	50.1	17.5
E6	50	54.2	14.2
N1	75	79.5	20.7
N2	63	87.0	28.9

the polymer particles as the reaction progresses. The number of particles formed by the surfactant remains constant and the size of the particles increases with time. That is a typical case of a micelle nucleation mechanism of particle formation in emulsion polymerization. The presence of a water-soluble comonomer results in a simultaneous homogeneous nucleation of particles. The water-soluble oligomers formed of NaSS can either be adsorbed on the particle surface and subsequently copolymerize with styrene and DVB or they can further polymerize to form homopolymer. This may produce a broad particle size distribution. The emulsifier-free synthesis demonstrates that the NaSS oligomers stabilize the polymer particles by forming copolymer with styrene and DVB. This is evident from the fact that the particles formed by the end of the reaction were stable in water and had the capacity to exchange Na$^+$ ions; this is explained in more detail in sections 3.2 and 3.3.

Agglomeration of the particles was evident in the images shown in Figure 2, especially for samples E2 and E4 made with 4% NaSS in the feed. As discussed earlier, NaSS forms an ionic charge on the particle surface which can repel the particles and prevent agglomeration. With only 4% NaSS in the feed, the ionic charge

may be inadequate to prevent agglomeration. Turner et al.[22] showed that NaSS incorporation in the copolymer increased as the amount of NaSS in the feed increased, and for 4 wt % NaSS in feed, less than 3 wt % of it was actually incorporated into the polymer. It was also observed that these polymer particle dispersions were very difficult to precipitate in methanol, which led us to perform dialysis followed by drying as a means of isolating free polymer nanoparticles.

TEM images of cross-linked polystyrene samples synthesized without emulsifier (N1 and N2) are shown in Figure 4, and particle sizes are listed in Table 2. The synthesis by the emulsifier-free polymerization procedure resulted in particles of much higher diameter compared to emulsion polymerization synthesis. The distribution became broader, and some secondary particles of much smaller size were also observed. The formation of secondary particles, reported in a similar work by Kim et al.,[25] can be attributed to the occurrence of both homogeneous and micelle nucleation. Two possible reasons related to molecular weight buildup can be proposed for the observed increase in particle size in this type of synthesis. First, the reaction times for these syntheses were much longer (42 h for N1 and 21 h for N2) compared to emulsion polymerization (6 h), which provided more time for the polymer particles to increase in size. The second reason, which applies mainly to N2, is that the concentration of NaSS monomer was increased in the feed in order to have an emulsifying effect, which may have produced higher molecular weight polymer through homogeneous nucleation.

3.2. FT-IR. The FT-IR absorbance spectra of the polystyrene particles prepared with various feed compositions are shown in Figure 5. The important absorption peak assignments are listed in Table 3. The peak at 1600 cm^{-1}, which corresponds to the C−C in-plane stretching of the styrene ring,[32] was used as an internal standard to normalize all the spectra. The broad peak at 3446 cm^{-1} results from O−H stretching vibrations in both residual water as well as the SO$_3$H group. The peaks in the range of 2800−3100 cm^{-1} represent various vibration bands of polystyrene.[32] The sharp peak around 697 cm^{-1} is the out-of-plane bending vibration of the styrene ring. Yang et al.[33] reported that the peak around 756 cm^{-1} is characteristic of the out-of-plane bending vibration of C−H groups in the monosubstituted benzene ring. In samples E2 and E4, small peaks are visible in the range of 1000−1200 cm^{-1}, and in samples E3 and E5, these peaks are well developed with higher intensities. The peak around 1040 cm^{-1} represents the symmetric stretching vibration of the SO$_3$ group and the relatively broad peak around 1182 cm^{-1} represents the asymmetric vibration of the SO$_3$ group. The normalized
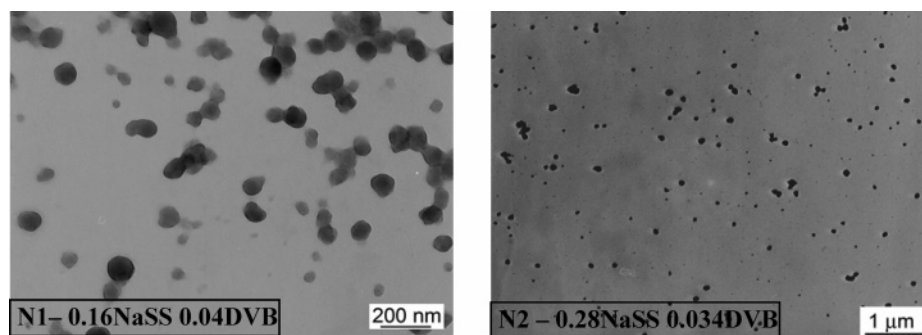

Figure 4. TEM images of cross-linked polystyrene nanoparticles synthesized with 20% and 40% NaSS and no emulsifier in the feed.
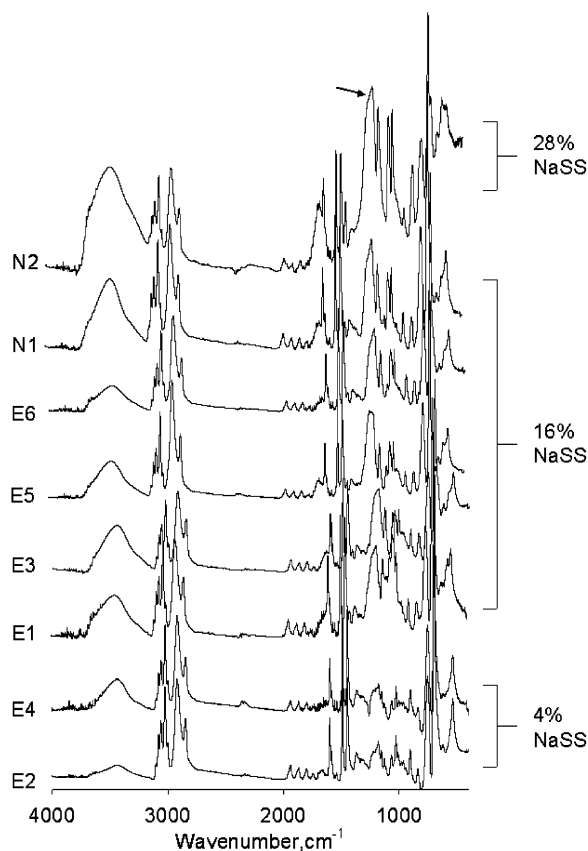
Figure 5. FTIR absorption spectra of polystyrene samples with feed composition E1, 0 DVB 0.167 NaSS; E2, 0.024 DVB 0.04 NaSS; E3, 0.021 DVB 0.163 NaSS; E4, 0.046 DVB 0.04 NaSS; E5, 0.04 DVB 0.16 NaSS; E6, 0.08 DVB 0.15 NaSS; N1, 0.04 DVB 0.16 NaSS; N2, 0.034 DVB 0.276 NaSS.

Table 3. Infrared Absorption Peak Assignments for Polystyrene

peak position, cm^{-1}	group
3446	O−H stretching
2900−2950	CH$_2$ stretchings
2800−3100	polystyrene stretching bands
1600	C−C in-plane stretching of ring
1041	S=O symmetric stretching
1182	S=O asymmetric stretching
834	C−H out-of-plane vibration for para position
756	C−H out-of-plane bending
697	phenyl out-of-plane bending

peak intensities at 1041 and 1182 cm^{-1} for all the samples are listed in Table 4. It is clearly evident that samples E3 and E5, made from 0.16 weight fraction of NaSS in the feed have sodium sulfonate groups on the phenyl ring, whereas in samples E2 and E4 made from 0.04 weight fraction of NaSS, the resonance could not be detected. Yang et al.[33] reported that the peak at 834 cm^{-1} corresponds to the C−H out-of-plane vibration for a para-substitution of the ring, and its intensity decreased with increasing SO$_3$ substitution. In our results, there is no indication of intensity change with respect to feed composition. This is expected because the para position of the phenylene ring is substituted with either the sodium sulfonate group or with another phenylene ring due to cross-linking.

3.3. Ion Exchange Capacity. The ion exchange capacity (IEC) gives a direct measure of the amount of NaSS incorporated in the polystyrene particles during the reaction. The IECs of the samples are listed in Table
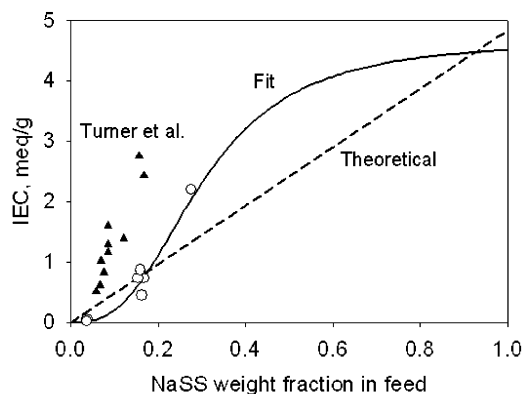

Figure 6. Effect of the NaSS weight fraction in comonomer feed on the ion exchange capacity of the final product. The open circles represent average experimental data for each preparation; curve fitted using $y = y_1 \times (x/0.3)^{2.8}/1.035 \times (1 + (x/0.3)^{2.8})$; dashed line represents theoretical IEC calculated from weight fraction of NaSS.

Table 4. Ion Exchange Capacity and Normalized IR Absorbance Intensity of Sulfonate Groups of Polystyrene Nanoparticles

			normalized IR absorbance intensity of S=O group	
sample ID	NaSS wt fraction	ion exchange capacity, meq/g	symmetric ($I_{1041 \text{ cm}^{-1}}$/ $I_{1600 \text{ cm}^{-1}}$)	asymmetric ($I_{1182 \text{ cm}^{-1}}$/ $I_{1600 \text{ cm}^{-1}}$)
E1	0.167	0.733	0.154	0.113
E2	0.038	0.059	0.041	0.067
E3	0.163	0.450	0.105	0.142
E4	0.037	0.024	0.033	0.065
E5	0.160	0.861	0.103	0.153
E6	0.154	0.733	0.109	0.145
N1	0.160	0.871	0.094	0.135
N2	0.276	2.197	0.164	0.196

4. Samples made with a 0.04-wt fraction NaSS in the feed have an IEC of 0.06 (E2) and 0.02 (E4) meq/g. As the NaSS wt fraction in the feed was increased to 0.16, the samples had an IEC in the range of 0.45−0.87 meq/g. An IEC close to the estimated value of 2.02 meq/g was attained when the wt fraction of NaSS in the feed was 0.28. The change in the amount of DVB in the feed did not significantly affect the IEC of our samples. This is evident from the results of the samples with ~16 wt % NaSS in the feed and varying amounts of DVB (E1, E3, E5, E6, and N1). The effect of NaSS weight fraction in the feed on the final IEC of the product is depicted in Figure 6. Although one would expect IEC to be linearly dependent on wt fraction of NaSS, the statistical analysis revealed that there was significant curvature in the data. It followed the following trend

$$y = \frac{y_1(x/0.3)^{2.8}}{1.035(1 + (x/0.3)^{2.8})} \qquad (2)$$

where y = ion exchange capacity, meq/g, x = weight fraction of NaSS.

This function was fitted by assuming a maximum theoretical IEC with 100% NaSS in the feed, which was calculated from

$$y_1 = \text{IEC}_{\text{max}}, \text{meq/g} = 10^{-3}/\text{mol.wt of NaSS} = 4.831$$

Each parameter for this function was found to be significant with $p < 0.0001$. The proposed model and experimental observations indicate that the entire

amount of NaSS in the feed is not incorporated in the final polymer. This was also reported by Turner et al.,[22] whose data are also plotted in Figure 6. In the initial part of the curve with weight fraction of NaSS less than 0.15, the amount of NaSS in the final polymer is less than the theoretical value. This suggests that there is predominantly micelle nucleation of polymer particles and the NaSS monomers or oligomers from the solution are not incorporated in the particles to the expected extent. As the weight fraction of NaSS increases in the feed, the conversion of the NaSS monomer into polymer also increases until a maximum is attained for a weight fraction of NaSS in feed of 1. This is evident from comparison with the theoretical IEC (also shown in Figure 6). The higher NaSS weight fraction increases the probability of homogeneous nucleation due to its solubility in water. As a result, more oligomers or polymer molecules of NaSS are incorporated into the particles. While the IEC observed by Turner et al. was much higher for a given weight fraction compared to our results, this discrepancy could be explained by the use of a cross-linking monomer in our system and/or differences in measurement of the IEC in the two studies. Turner et al. relied on elemental analysis to find the IEC. Measurement of IEC by titration leads to recognition of only exchangeable $-SO_3Na$ groups, and perhaps some of the groups buried inside the particles were not accessible to the reagents, especially at low IEC.

4. Conclusion

Cross-linked polystyrene nanoparticles in the size range of 40−80 nm were synthesized by emulsion polymerization. NaSS was used as a stabilizing comonomer, and DVB was used as a cross-linking agent. Synthesis of particles by emulsifier-free technique resulted in the formation of particles in the size range of 70−80 nm. The particles had broad size distribution which could be attributed to dual nucleation mechanism due to the presence of large amounts of surface active agents. The IEC of particles increased with increasing amounts of NaSS in the feed. The sulfonation data could be explained by a sigmoidal function of the concentration of NaSS in the feed. A maximum IEC of 2.2 meq/g was attained by incorporating 0.28-weight fraction NaSS in the feed. The particle size increased with increasing amounts of DVB in the feed. The method of emulsifier-free synthesis offers an advantage over emulsion polymerization in that the emulsifier is eliminated from the final product without compromising on the particle size. Due to the presence of NaSS as a comonomer, these particles have an ion exchange capacity and can be used in various applications. The presence of ionic monomer also seemed to have reduced the apparent aggregation of particles in water.

Literature Cited

(1) Aoki, S.; Otsu, T.; Imoto, M. Cationic polymerization of isobutyl vinyl ether catalyzed by ion-exchange resin [poly(styrenesulfonic acid)]. *Makromol. Chem.* **1966**, *99*, 133.

(2) Ghanem, N. A.; Moustafa, A. B.; Mohsen, R. *n*-Butyl methacrylate from methyl methacrylate by transesterification using an ion-exchange resin as catalyst. *Chem. Ind. (London, UK)* **1971**, 513.

(3) Koyama, K.; Otsu, T. Polymerization of 1,3-dioxolane catalyzed by ion-exchange resin (polystyrene sulfonic acid). *J. Macromol. Sci., Chem.* **1974**, *A8*, 1295.

(4) Kim, J. H.; El-Aasser, M. S.; Klein, A.; Vanderhoff, J. W. Sulfonated latex particle as acid catalysts for the continuous inversion of sucrose. *J. Appl. Polym. Sci.* **1988**, *35*, 2117.

(5) Djinovic, V. M.; Antic, V. V.; Djonlagic, J.; Govedarica, M. N. Synthesis of a,w-dicarboxypropyl oligodimethylsiloxanes by ion-exchange resin catalyzed equilibration polymerization. *React. Funct. Polym.* **2000**, *44*, 299.

(6) De Lucas, A.; Canizares, P.; Rodriguez, J. F. Removal of alkaline catalysts from polyols by ion exchange: selection of an ion-exchange resin. *Separ. Sci. Technol.* **1995**, *30*, 125.

(7) Matyjaszewski, K.; Pintauer, T.; Gaynor, S. Removal of Copper-Based Catalyst in Atom Transfer Radical Polymerization Using Ion Exchange Resins. *Macromolecules* **2000**, *33*, 1476.

(8) Malini, K. A.; Anantharaman, M. R.; Sindhu, S.; Chinnasamy, C. N.; Ponpandian, N.; Narayanasamy, A.; Balachandran, M.; Pillai, V. N. S. Effect of cycling on the magnetization of ion exchanged magnetic nanocomposite based on polystyrene. *J. Mater. Sci.* **2001**, *36*, 821.

(9) Boardman, N. K. Chromatography of proteins on Celite ion-exchange resins. II. Chromatography of insulin on a Celite-sulfonic acid ion-exchange resin. *J. Chromatogr.* **1959**, *2*, 398.

(10) Hanai, T.; Walton, H. F. Chromatography of chlorinated biphenyls on an ion-exchange resin. *Anal. Chem.* **1977**, *49*, 764.

(11) Hong, L.; Chen, N. Proton-conducting polymer membrane based on sulfonated polystyrene microspheres and an amphiphilic polymer blend. *J. Polym. Sci. Polym. Phys.* **2000**, *38*, 1530.

(12) Chen, N.; Hong, L. Proton-conducting membrane composed of sulfonated polystyrene microspheres, poly(vinylpyrrolidone) and poly(vinylidene fluoride). *Solid State Ionics* **2002**, *46*, 377−385.

(13) Chen, N.; Hong, L. Embedding poly(styrene sulfonic acid) into PVDF matrix-a new type of proton electrolyte membrane. *Polymer* **2004**, *45*, 2403.

(14) Chen, S.-L.; Krishnan, L.; Srinivasan, S.; Benziger, J.; Bocarsly, A. B. Ion-exchange resin/polystyrene sulfonate composite membranes for PEM fuel cells. *J. Membr. Sci.* **2004**, *243*, 327.

(15) Oren, Y.; Fregen, V.; Linder, C. Highly conductive ordered heterogeneous ion-exchange membranes. *J. Membr. Sci.* **2004**, *239*, 17.

(16) Chan, F. S.; Goring, D. A. I. Preparation and characterization of sulfonated polystyrene latexes. *Can. J. Chem.* **1966**, *44*, 725.

(17) Lenzi, M. K.; Silva, F. M.; Lima, E. L.; Pinto, J. C. Semibatch styrene suspension polymerization processes. *J. Appl. Polym. Sci.* **2003**, *89*, 3021.

(18) Barar, D. G.; Staller, K. P.; Peppas, N. A. Friedel−Crafts cross-linking methods for polystyrene modification. 3. Preparation and swelling characteristics of cross-linked particles. *Ind. Eng. Chem. Prod. R&D* **1983**, *22*, 161.

(19) Berlin, A. A.; Gil'man, I. M. Styrene suspension polymerization. *Khim. Prom.* **1957**, 449.

(20) Hauser, E. A.; Perry, E. Emulsion polymerization of styrene. *J. Phys. Colloid Chem.* **1948**, *52*, 1175.

(21) Odian, G. *Principles of Polymerization*, 3rd ed.; John Wiley & Sons: New York, 1991.

(22) Turner, S. R.; Weiss, R. A.; Lundberg, R. D. The emulsion copolymerization of styrene and sodium styrene sulfonate. *J. Polym. Sci. Polym. Chem. Ed.* **1985**, *23*, 535.

(23) Aslamazova, T.; Tauer, K. On the colloidal stability of polystyrene particles prepared with surface-active initiators. *Adv. Colloid Interface Sci.* **2003**, *104*, 273.

(24) Okubo, M.; Yamada, A.; Shibao, S.; Nakamae, K.; Matsumoto, T. Studies on suspension and emulsion. XLVI. Emulsifier-free emulsion polymerization of styrene in acetone−water. *J. Appl. Polym. Sci.* **1981**, *26*, 1675.

(25) Kim, J. H.; Chainey, M.; El-Aasser, M. S.; Vanderhoff, J. W. Emulsifier-free emulsion copolymerization of styrene and sodium styrene sulfonate. *J. Polym. Sci. Polym. Chem.* **1992**, *30*, 171.

(26) Xu, X.-J.; Siow, K.-S.; Wong, M.-K.; Gan, L.-M. Polymerization of styrene with ionic comonomer, nonionic comonomer, or both. *J. Polym. Sci. Polym. Chem.* **2001**, *39*, 1634.

(27) Zeng, F.; Sun, Z.; Wu, S.; Liu, X.; Wang, Z.; Tong, Z. Preparation of highly charged, monodisperse nanospheres. *Macromol. Chem. Phys.* **2002**, *203*, 673.

(28) Bai, F.; Yang, X.; Huang, W. Synthesis of Narrow or Monodisperse Poly(divinylbenzene) Microspheres by Distillation-Precipitation Polymerization. *Macromolecules* **2004**, *37*, 9746.

(29) Yang, W.; Ming, W.; Hu, J.; Lu, X.; Fu, S. Morphological investigation of cross-linked polystyrene microspheres by seeded polymerization. *Colloid Polym. Sci.* **1998**, *276*, 655.

(30) Smith, W. V. The kinetics of styrene emulsion polymerization. *J. Am. Chem. Soc.* **1948**, *70*, 3695.

(31) Ewart, R. H.; Carr, C. I. The distribution of particle sizes in polystyrene latex. *J. Phys. Chem.* **1954**, *58*, 640.

(32) Bhutto, A. A.; Vesely, D.; Gabrys, B. J. Miscibility and interactions in polystyrene and sodium sulfonated polystyrene with poly(vinyl methyl ether) PVME blends. Part II. FTIR. *Polymer* **2003**, *44*, 6627.

(33) Yang, J. C.; Jablonsky, M. J.; Mays, J. W. NMR and FT-IR studies of sulfonated styrene-based homopolymers and copolymers. *Polymer* **2002**, *43*, 5125.